Discrete set selection of Saffman–Taylor fingers

David A. Kessler
Department of Physics, University of Michigan, Ann Arbor, Michigan 48109
Herbert Levine
Schlumberger–Doll Research, Old Quarry Road, Ridgefield, Connecticut 06877

(Received 11 August 1986; accepted 23 January 1987)

A study of the linear stability of the discrete set of steady-state Saffman–Taylor finger solutions at finite surface tension is presented. It is shown by explicit computation that members of the set aside from the lowest width finger are linearly unstable. This completes the demonstration that finite surface tension effects determine uniquely the allowed interfacial pattern in the steady-state regime.

I. INTRODUCTION

The problem of finger width determination for a multiphase interface in a Hele–Shaw cell has recently received renewed attention.[1] In particular, the continuous family of solutions found by Saffman and Taylor[2] has been shown[3] to break down to a discrete set upon introduction of a pressure drop due to surface tension at the fluid–fluid interface. This breakdown has been traced[4] to the presence of essentially singular terms which destroy interface smoothness at all but certain allowed widths $\{\lambda_i\}$. This idea, coined "microscopic solvability," has given rise[5] to analytic derivations of the scaling $(\lambda - \frac{1}{2}) \sim \gamma^{2/3}$ (where γ is the dimensionless surface tension defined below), as well as a new understanding as to why fingers remain stable up to large capillary numbers.[4]

The purpose of this article is to formulate a new computational approach to the linear stability of the finite surface tension steady-state solution. This new method makes use of the exact numerically determined finger shape and hence represents an improvement over some recent treatments.[4,6,7] The major result we wish to present is that we can unequivocally demonstrate the existence of discrete mode instabilities for certain elements of the allowed set aside from the smallest width finger. These results agree completely with the conjectures made by us in our earlier, approximate treatment.[4] This result then strongly suggests that only the narrowest finger can be linearly stable; this in turn means that only fingers with this width can be observed in either numerical simulations or laboratory experiments. The prediction made in this manner agrees with the simulations[8] and can be made to agree with the experiments upon taking into account effects of wetting films on the plates.[9]

The outline of this work is as follows. First, in Sec. II we derive the linear operator governing perturbations around the steady-state solution. Next, in Sec. III we describe our numerical procedure for studying this operator. Finally, in Sec. IV we present our results and introduce a conjecture as to the stability of the infinite discrete family of steady-state interfaces found originally by Vanden-Broeck.[3]

II. LINEAR STABILITY OPERATOR

The evolution equation for the interface in a Hele–Shaw cell is easy to derive. We start the usual formulation of a zero viscosity fluid displacing a viscous one: $\nabla^2 p = 0$, $(\partial p/\partial y)(y = \pm 1) = 0$, and $p(x \sim \infty) \sim -x$, together with the Stefan condition $-\nabla p \cdot n = v_n$ and the pressure jump $p_{\text{int}} = -\gamma\kappa$, where $\gamma = (T/12\mu v_\infty)(b^2/a^2)$ for surface tension T, viscosity μ, channel width $2a$, and gap thickness b, and where v_∞ is the asymptotic flow. Our coordinate system is given in Fig. 1. We can then eliminate the pressure field by using a Green's function for Laplace's equation in a channel geometry. This leads to

$$\int \hat{n}' \cdot \nabla' G(x,x',y,y')\gamma\kappa(s')ds' = \int G(x,x';y,y')v_n(s')ds', \tag{1}$$

where

$$G = -\tfrac{1}{2}\theta(x-x')|x-x'| - (1/4\pi)\log(1 + e^{-2\pi|x-x'|} - 2\cos\pi(y-y')e^{-\pi|x-x'|}), \tag{2}$$

where ds' is a unit of arc length, $\hat{n}$ is the curve normal, and we have assumed a symmetric profile. The singularity at $x = x'$ in the first term is regularized by approaching the interface from the nonviscous fluid side.

Equation (1) can be used to recover the results of Vanden-Broeck[3] for the emergence of a discrete set. Specifically, we choose a value of γ and solve for a shape that uniformly translates with velocity $1/\lambda$. It is easy to show that this shape must asymptotically approach $y = \pm\lambda$; we solve the flow equation in the gap between the wall and the finger by assuming

$$y_{\text{int}} = \lambda - e^{bx}, \quad \phi(x,y) = a\cos bye^{bx}.$$

Substitution into the equation of motion leads to the condition $\gamma b^2 \tan(b\lambda) = 1$ for the approach rate b. We then can parametrize the shape in any convenient manner and solve for the resulting unknowns by iteration. In general, such a solution of Eq. (1) has a cusp at the origin. The discrete set

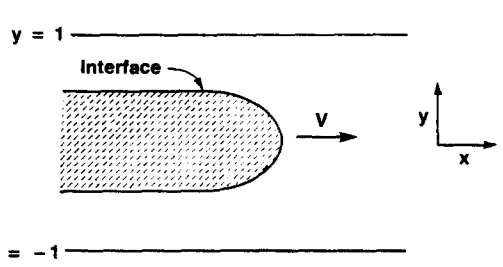

FIG. 1. Top view of Hele–Shaw geometry.

 0031-9171/87/051246-04$01.90

$\{\lambda\}$ is selected by imposing the auxiliary condition of vanishing cusp magnitude. The details of the implementation of this approach have been given elsewhere.[10] The results of our method agree with those found by the conformal mapping technique of Vanden-Broeck.[3] We prefer our methodology because it is immediately generalizable to systems that obey more complicated field equations for which conformal mapping is of no avail.

Once a steady-state solution has been found, we set $\mathbf{x}(s) = \mathbf{x}_0 + t/\lambda\hat{x} + \hat{n}\delta(t,s)$ and linearize in δ. We then have to compute a variety of expressions, determining how the various geometrical constructs in Eq. (1) change to first order in δ. Clearly, the Green's function must now be evaluated at the perturbed interface:

$$G(x,x',yy') = G(\cdot) + [\delta(s)\hat{n}\cdot\nabla + \delta(s')\hat{n}'\cdot\nabla']G(\cdot), \quad (3)$$

where $G(\cdot)$ is the Green's function at the unperturbed interface. Similarly, the curvature must be modified via

$$\kappa = \kappa_0 - \delta''(s) - \kappa_0^2\delta(s).$$

There are analogous expressions for the velocity

$$v_n = (1/\lambda)\cos\theta + \dot{\delta} + (1/\lambda)\sin\theta\delta',$$

where θ is the angle made by the normal vector to the propagation direction, the normal vector, and the arc length measure. A simple calculation leads to the linear equation

$$\begin{aligned}
&\int \hat{n}'\cdot\nabla'[\delta(s)\hat{n}\cdot\nabla + \delta(s')\hat{n}'\cdot\nabla']G(\cdot)\gamma\kappa_0(s')ds' \\
&\quad + \int \delta'(s')\hat{t}'\cdot\nabla'G(\cdot)\gamma\kappa_0^2(s')ds' \\
&\quad - \int \hat{n}'\cdot\nabla'G(\cdot)\gamma\delta''(s')ds' \\
&\quad = \int [\delta(s)\hat{n}\cdot\nabla + \delta(s')\hat{n}'\cdot\nabla']G(\cdot)ds'\,\hat{n}(s')\cdot\frac{\hat{x}}{\lambda} \\
&\quad + \int G(\cdot)\left(\dot{\delta}(s') - \frac{\hat{t}'\cdot\hat{x}}{\lambda}\delta'(s') + \kappa_0\delta(s')\right)ds', \quad (4)
\end{aligned}$$

where $\hat{t}$ is the tangent vector and κ_0 is the curvature of the steady-state interface.

We now wish to study modes at a single complex frequency ω. Schematically, Eq. (4) is of the form $A^{(1)}\delta = A^{(0)}(v^{[1]}[\delta])$, where $A^{(1)}$ and $A^{(0)}$ are linear integro-differential operators and $v^{[1]}[\delta] = \omega\delta - \hat{t}\cdot\hat{x}\delta'/\lambda + \kappa_0\delta$ for the mode at fixed frequency. It is important to note that $A^{(0)}$ is singular. The easiest way to see that this must be true is to recognize that the zero-mode problem for this operator is isomorphic to finding the charge distribution on a conductor of electrostatic potential $\phi = 0$. This just means that the velocity is not uniquely determined until we impose an additional constraint of the form

$$\int ds'\, v^{[1]}[\delta(s')] = 0,$$

which is just the condition that the perturbation not be allowed to change the flux asymptotically far downstream.

The above equation gives rise to both continuous and discrete modes of oscillation around the initial finger. The continuum corresponds to perturbations which asymptotically approach growing plane waves on the planar interface in the tail region of the finger. If we substitute the form $\delta = e^{ks_0}$ into Eq. (4), we find[4]

$$\omega = -k/\lambda - \gamma k^3\tan(k\lambda).$$

Because the above form gives negative growth rates for imaginary wave vectors, it is possible to show that the continuum is always stable.[4,7,11] The physical interpretation of this stability is that interface normal velocity goes to zero down the tail and therefore the perturbation amplitude is damped at large distances. This result can be explicitly verified using the numerical algorithm to be discussed below, but this is not our concern here.

The more interesting part of the spectrum is that of the discrete eigenvalues. These modes all decay exponentially away from the tip, as can be seen by noting that such modes are possible only if the contributions from the integral operators in (4) are *not* dominated by the contribution from far distances (see Ref. 4 for an explicit derivation). Because of this, these modes avoid the previous arguments for stability and may give rise to tip-region instabilities. The remainder of this work will focus on a numerical study of this type of mode.

III. NUMERICAL METHOD

We wish to study the spectrum of the operator implicitly defined by the linear equation derived in Sec. II. We start by defining a mesh variable $u_i = iu_{\max}/\mathrm{NPTS}$, in terms of which the independent variable y is given by $y_i = (2\lambda/\pi)\tan^{-1}\sinh u_i$. (NPTS is the number of points in the numerical discretization.) Similarly, we denote $x_i \equiv x_0(y_i)$. The unknown function is then determined by the finite number of unknowns $\delta_i = \delta(s_0(y_i))$, where the arc length function s_0 is directly determined from the initial steady-state solution. By its construction, u is proportional to the arc length at large distances and our mesh becomes one of equal spacing in the arc length. We explicitly require the eigenvectors to vanish for distances larger than the spatial cutoff $u_{\max}$. This introduces some inaccuracy in the continuum modes (see below), but, as we shall explicitly check later, does not affect any discrete modes corresponding to possible tip-region instabilities.

The derivative terms are discretized by simple three-point expressions. After accounting for delta function pieces which can be trivially integrated, all the integrals entering into $A^{(1)}$ are *nonsingular* at $s = s'$ and simple trapezoidal rule discretization is accurate to $O(1/\mathrm{NPTS}^2)$. The integrand comprising $A^{(0)}$ is logarithmically singular and must be handled more carefully. We use

$$\begin{aligned}
\int G(\cdot)v^{[1]}[\delta(s')] &= \int G(\cdot)\{v^{[1]}[\delta(s')] - v^{[1]}[\delta(s)]\} \\
&\quad + v^{[1]}[\delta(s)]\int G(\cdot)
\end{aligned}$$

and then replace

$$\int G(\cdot) = \lambda\int \hat{n}'\cdot\nabla'G(\cdot)\gamma\kappa(s')ds'$$

via the steady-state equation. This method is again accurate to $O(1/\mathrm{NPTS}^2)$.

Once the matrices $A^{(1)}$ and $A^{(0)}$ are computed, we define

TABLE I. Typical data set, fit by $\omega = 0.0015 + 96.75(u_{max}/\text{NPTS})^2$, for $u_{max} \geqslant 5$.

u_{max}	NPTS	MPTS	$\omega(\times 10^{-2})$
4.0	200	100	4.238
5.0	200	100	6.197
7.5	300	150	6.185
5.0	300	150	2.839
5.0	400	200	1.666
5.0	300	100	2.839
5.0	300	200	2.839

TABLE II. Raw data for the unstable mode on the second solution branch; the extrapolated eigenvalue occurs at $\omega = 2.11$.

u_{max}	NPTS	MPTS	ω
4.0	200	100	2.183
5.0	200	100	2.223
7.5	300	150	2.223
5.0	300	150	2.160
5.0	400	200	2.138
5.0	300	100	2.160
5.0	300	200	2.160

an operator $L = (A^{(0)})^{-1}A^{(1)}$. As already mentioned, $A^{(0)}$ is singular and the inversion must be done via the imposition of the flux constraint. It is easy to prove that $A^{(1)}$ is orthogonal to the zero mode and hence no ambiguity arises in this procedure. Finally, we define

$$\tilde{L}[\delta] = L[\delta] + \hat{t}\cdot\hat{x}\delta' - \kappa_0\delta$$

as the linear stability operator.

In order to minimize boundary effects, we truncate to a MPTS$\times$MPTS submatrix of $\tilde{L}$. In practice, we usually take MPTS $= \frac{1}{2}$NPTS, but larger fractions (up to 75%) are equally effective. This submatrix truncation effectively amounts to including contributions to the integrals in (4) from distant regions (large s') without having to explicitly parametrize the eigenvector in that domain. One can show that without this additional contribution, there can be large power-law corrections $[O(1/u_{max})]$ to some of the eigenvalues and that for fixed MPTS, increasing NPTS improves the convergence. (In any event, none of our conclusions depend in any way on the details of this procedure.) Finally, then, any specific calculation is characterized by the triple (MPTS, NPTS, and u_{max}) and the physical numbers must be found by extrapolation to infinite values of these cutoff parameters.

We know *a priori* that there must be at least one discrete mode occurring at exactly $\omega = 0$ due to translation invariance. One major test of our method is its ability to reproduce this $\omega = 0$ mode; this mode is *not* decoupled from the remainder of the matrix[12] and its value will accurately reflect numerical errors in our cutoff procedure. To do this, we first generated a 150-point solution of the steady-state equation corresponding to

$$\gamma = 5.724\times 10^{-3}, \quad \lambda = 0.52375 \pm 5\times 10^{-5}.$$

Then we computed the spectrum by using the EISPACK[13] nonsymmetric matrix routine with various values of the cutoff parameters. A typical data set is presented in Table I. Our procedure was to choose u_{max} large enough such that its variation did not affect the desired eigenvalue more than 0.25%. This can always be done for any mode whose corresponding eigenvector decays rapidly away from the tip. Then, we increase the spatial resolution u_{max}/NPTS and check that the data agree with the quadratic convergence expected of our algorithm. This then allows us to present the final extrapolated value for the discrete eigenvalue. Finally we check that this eigenvalue is independent of the ratio MPTS/NPTS.

Using the above procedure, the numerical value of the zero mode was extrapolated to be $\omega_0 = 1.5\times 10^{-3}$, a factor of 5×10^3 *smaller* than any other mode. This then is a measure of the accuracy of our method.

IV. TIP-REGION INSTABILITIES

Let us return to the same solution as we have just used for our accuracy test. To go further, we apply the same procedure to the other discrete modes of the system. At this steady-state solution, there is only one other discrete mode, $\omega = -4.55$. With respect to these excitations, then, the finger is linearly stable. As stated above, all the continuum modes for this solution are also stable. This finger is therefore linearly stable, at least with respect to symmetric perturbations.

The case of (γ,λ) just considered corresponds to the smallest allowed width at that value of γ. We now turn to different allowed λ values at constant γ. The next root occurs at $\lambda = 0.5945$. Again, there is a translation mode whose value even for the lowest precision runs never exceeds 10^{-1} and can be extrapolated to equal 10^{-3} at infinite spatial resolution. The other discrete modes are now at $\omega = +2.11$ and -3.78. Table II contains our raw data for the different cutoffs that entered into determining the unstable mode eigenvalue. Our data prove that there is a discrete mode instability that prevents this width from ever being observed experimentally! The eigenvalue again shows no u_{max} dependence (at fixed resolution) and as expected, the eigenvector decays exponentially away from the tip region. In

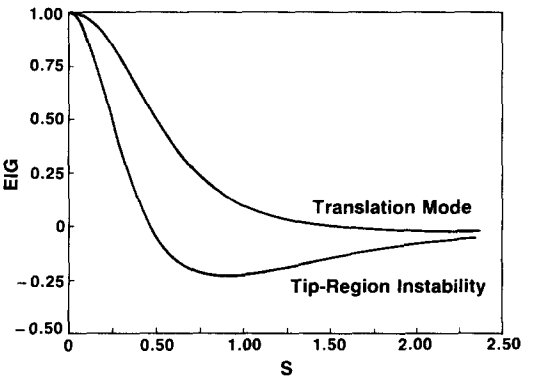

FIG. 2. Eigenvectors corresponding to translation mode (upper) and tip-region instability (lower) versus arc length from the tip.

Fig. 2 we have plotted this eigenvector as well as the translation mode eigenvector in the tip region.

The picture at all other values of γ which we studied to date is identical. For example, we present results for $\gamma = 0.003$. The lowest root occurs at $\lambda = 0.5148$ and has no discrete modes other than the omnipresent translation mode. The second solution now has width $\lambda = 0.5587$ and modes at 2.4, 0, and -4.1. Again, the second solution has one unstable mode.

What happens when we go to higher width solutions? We have studied the third root at $\gamma = 5.724 \times 10^{-3}$ which occurs at $\lambda = 0.705$. The qualitative features of the spectrum remain unchanged and the discrete modes now occur at $\omega = \{4.36, 1.77, 0, -3.38\}$. Now there are *two* unstable discrete modes. We have tested this at other values of γ with the same result. The sum of our numerical results provide what we feel is strong evidence for the following scenario: As λ is increased for fixed γ, we pass through a discrete set of allowed values; each additional steady-state solution has one additional unstable mode. As we reach $\lambda = 1$, we go over to the stability of a planar interface, as originally given by Saffman and Taylor.[2] Similarly, as γ is decreased at fixed λ, we likewise go through a series of solutions and again each additional solution has one additional instability. As we reach $\gamma = 0$, the discrete spectrum goes over to the $\gamma = 0$ spectrum of McLean and Saffman.[14] Clearly, however, only an analytic approach can ever actually prove that this is indeed what happens.

Finally, we note that this sort of spectral flow theorem is not restricted to the Saffman–Taylor finger. In a separate work,[15] we have shown that this exact scenario appears to be valid for diffusion-controlled dendritic crystal growth. The emergence of a discrete set in both of these systems, as well as some others such as Taylor bubbles and directional solidification, has been understood by the working of "microscopic solvability." In a way in which we do not yet fully understand, this type of mechanism for pattern selection also ensures that only one steady-state solution can be linearly stable and hence predicts a *unique* pattern for the evolution of the phase boundary.

ACKNOWLEDGMENT

The work of one of us (DK) was supported by DOE Grant No. DE-FG-02-85ER54189.

[1]For a recent review, see D. Kessler, J. Koplik, and H. Levine, submitted to Adv. Phys.
[2]P. G. Saffman and G. I. Taylor, Proc. R. Soc. London Ser. A **245**, 312 (1958).
[3]J. M. Vanden-Broeck, Phys. Fluids **26**, 2033 (1983).
[4]D. Kessler and H. Levine, Phys. Rev. A **33**, 2621, 2634 (1986).
[5]B. I. Shraiman, Phys. Rev. Lett. **56**, 2028 (1986); R. Combescot, T. Dombre, V. Hakim, Y. Pomeau, and A. Pumir, *ibid.* **56**, 2036 (1986); D. Hong and J. Langer, *ibid.* **56**, 2032 (1986).
[6]D. Kessler and H. Levine, Phys. Rev. A **32**, 1930 (1985).
[7]D. Bensimon, Phys. Rev. A **32**, 1302 (1986).
[8]L. Schwartz and A. J. DeGregorio, J. Fluid Mech. **164**, 383 (1986); G. Trygvasson and H. Aref, *ibid.* **136**, 1 (1983).
[9]P. Tabeling, G. Zocchi, and A. Libchaber, J. Fluid Mech., in press.
[10]D. Kessler, J. Koplik, and H. Levine, Phys. Rev. A **34**, 4980 (1986).
[11]P. Pelce, Ph.D. thesis, Universite de Provence, France, 1986; D. Bensimon, L. Kadanoff, S. Liang, B. Shraiman, and C. Tang, Rev. Mod. Phys. **58**, 977 (1986).
[12]This decoupling occurs, for example, in the method used in Ref. 7.
[13]B. T. Smith, in *Matrix Eigensystem Routines—EISPACK Guide, Lecture Notes in Computer Science*, Vol. 6, edited by G. Goos and J. Hartmanis (Springer, New York, 1974).
[14]J. W. McLean and P. G. Saffman, J. Fluid Mech. **102**, 455 (1981).
[15]D. Kessler and H. Levine, Phys. Rev. Lett. **57**, 3069 (1986).